

Nano/macro-hardness and fracture resistance of $\text{Si}_3\text{N}_4/\text{SiC}$ composites with up to 13 wt.% of SiC nano-particles

M. Balog^{a,*}, J. Kečkéš^b, T. Schöberl^b, D. Galusek^c, F. Hofer^d, J. Křest'an^a,
Z. Lenčéš^a, J.-L. Huang^e, P. Šajgalík^a

^a Institute of Inorganic Chemistry, Slovak Academy of Sciences, Bratislava, Slovakia

^b Erich Schmid Institute for Materials Research, Austrian Acad. Sciences, Leoben, Austria

^c VitrumLaugaricio, Joint Glass Centre of the Institute of Inorganic Chemistry SAS, Alexander Dubček University of Trenčín, and RONA, a.s., Trenčín, Slovakia

^d Research Institute for Electron Microscopy and Fine Structure, University of Technology, Graz, Austria

^e Department of Materials Science and Engineering, National Cheng Kung University, Tainan, Taiwan, ROC

Received 2 April 2006; received in revised form 1 August 2006; accepted 7 August 2006

Available online 17 October 2006

Abstract

Relations between composition and mechanical properties of the $\text{Si}_3\text{N}_4/\text{SiC}$ micro/nano-composites were studied by combination of nano-indentation and Vickers indentation techniques. The $\text{Si}_3\text{N}_4/\text{SiC}$ composites were prepared from crystalline Si_3N_4 powder doped with SiNC amorphous precursor and yttria as the sintering aid. During sintering the SiNC precursor crystallised to yield both SiC and Si_3N_4 . The *in situ* formed SiC particles were located both *inter*- and *intra*-granularly. The presence of SiC nano-particles enhanced the nano- and macro-hardness, and the fracture toughness of the composites. The nano-hardness of $\text{Si}_3\text{N}_4/\text{SiC}$ composites ranged between 20 and 24 GPa, and depends on the volume fraction of SiC. The nano-hardness of individual Si_3N_4 grains exhibited large scatter as the consequence of the presence of *intra*-SiC inclusions, which directly influence the measured values as the harder phase, or by generating large thermal stresses within Si_3N_4 grains. Consequently the scatter of nano-hardness was much larger than in case of macro-hardness where the measured values are averaged over large area. The nano-indentation of grain boundaries indicates that the boundaries are much softer than the surrounding matrix phase. Apart of indentation size effect (ISE) this is believed to be an additional reason why the measured values of macro-hardness are lower than the nano-hardness. The maximum fracture toughness ($5.8 \text{ MPa m}^{1/2}$) was achieved for the composite with the total amount of 8 wt.% SiC, where a percolating network of intergranular SiC particles was formed, as indicated by the measurement of electrical resistivity.

© 2006 Elsevier Ltd. All rights reserved.

Keywords: Si_3N_4 ; SiC; Hardness; Nano-hardness; Toughness and toughening; Nanocomposites

1. Introduction

Owing to their good mechanical properties the modern advanced ceramics are the materials of interest for various engineering applications. The recent trends in materials engineering favour composite materials against the more traditional monolithic ceramics. The new kind of ceramic composites called nano-composites, exhibit improved properties compared with “pure” monolithic ceramics. Successful preparation of advanced composites of $\text{Si}_3\text{N}_4/\text{TiN}$,^{1,2} $\text{Si}_3\text{N}_4/$

SiC ,^{3–5} $\text{Al}_2\text{O}_3/\text{SiC}$,⁶ TiC/SiC ^{7,8} and many others have been reported.

Promising candidates for advanced applications are $\text{Si}_3\text{N}_4/\text{SiC}$ micro/nano-composites. Doping of the starting Si_3N_4 powder with amorphous SiNC precursor was reported as a suitable route of preparation of such materials.⁹ During sintering the amorphous SiNC crystallises, and yields SiC and Si_3N_4 . Other perspective route for preparation of “low cost” $\text{Si}_3\text{N}_4/\text{SiC}$ composites is the addition of silica and carbon into the starting powder mixture.¹⁰ Silica reacts with carbon, and the carbothermal reduction yields the desired SiC. In both cases the *in situ* formed SiC particles are located in two positions: within the Si_3N_4 grains (*intra*-particles) and at grain boundaries (*inter*-particles).^{10,11}

* Corresponding author.

E-mail address: uachbalo@savba.sk (M. Balog).

Owing to the presence of SiC inclusions the composites exhibit improved mechanical properties at room and elevated temperatures. Especially, remarkable improvement of creep resistance was observed.⁹ The presence of *inter*-SiC particles at Si₃N₄ grain boundaries and in triple pockets increases the internal friction on grain boundaries by grain boundary pinning. Moreover, residual carbon changes the chemistry of glassy phase. Carbon reacts with silica, which depletes the glassy phase of SiO₂ and shifts the composition of residual glass from nearly eutectic to compositions with higher melting temperature.

The mechanisms, how the *intra*-SiC particles influence the mechanical properties of Si₃N₄/SiC micro/nano-composite are still discussed. Nano-indentation appears to be a useful tool for investigation of the direct influence of SiC particles in nano-composites on mechanical properties, owing to the possibility of direct characterisation of interior part of micrometer sized matrix grains with dispersed nanophase.¹² As a consequence the influence of *intra*-inclusions on macro-mechanical properties can be estimated.

The present work attempts to use nano-indentation combined with standard hardness measurements as a way to elucidate the influence of SiC nano-inclusions on the hardness and fracture toughness of Si₃N₄/SiC composites.

2. Experimental

Si₃N₄ powder (UBE Industries, Ltd., Japan, grade SN-E10) was mixed with Y₂O₃ (H.C. Starck, Germany, grade F) and amorphous SiNC powder. The SiNC amorphous powder was prepared by pyrolysis of polysilazane based precursor NCP 200 (Nichimen, Japan) at TU Darmstadt as a microstructure modifying additive. The chemical compositions of the studied samples are listed in Table 1. The powder mixtures were attrition milled in isopropanol for 4 h. The dried powders were sieved through 25 µm mesh screen to remove agglomerates. Samples were uniaxially pressed in a steel die at 100 MPa pressure in order to prepare the cylindrical pellets with the diameter of 12 and 10 mm height. Green bodies were embedded into BN and hot-pressed at 1750 °C for 1 h under slight overpressure of nitrogen (0.12 MPa) and with 30 MPa load.

The densities of samples were measured by Archimedes method in mercury. The theoretical densities were calculated according to the rule of mixtures. For the microstructure anal-

yses the hot-pressed materials were cut, polished, and plasma etched with CF₄ + O₂ gas mixture. The microstructures were examined by scanning electron microscopy (SEM, Zeiss, EVO 40) and by transmission electron microscopy (TEM). Analytical transmission electron microscopy was performed using a Gatan imaging filter mounted on a Philips CM20 TEM/STEM (acceleration voltage 200 kV, equipped with LaB₆ cathode). The Si₃N₄-SiC composite of thickness 100 µm was dimpled to a thickness of about 20 µm. The thin foil was then ion-milled until perforation.^{13,14} Chemical analyses were carried out by electron dispersive X-ray analysis (EDX) and electron energy loss spectroscopy (EELS), respectively.

Macro-hardness was determined using Vickers indentation method (LECO Hardness Tester, Model LV-100AT) at the load of 9.81 N. Nano-hardness was determined by depth sensing quasi-static tests on a Hysitron Triboscope mounted on the scanner head of a DI (Veeco) Dimension 3100 atomic force microscope (AFM) using the Berkovich indenter. This device allows positioning of the indents with an accuracy of <20 nm. Due to very small size and depth of indents the preliminary nano-hardness measurements were for all compositions influenced by the surface characteristics of tested specimens. Systematic study of the applied load versus nano-hardness showed the loading of 2.0 mN as the optimum load for elimination of this effect. At this load the influence of the surface layer on the measured hardness values was negligible, and crack formation was not yet observed. Each sample was indented more than 70 times, and the imprints in the vicinity of microstructural defects (pores, removed grains, etc.) were excluded from the evaluation of measured data. Fracture toughness was determined by indentation method at the load of 98.1 N, and calculated by the method described by Shetty et al.¹⁵ Electrical resistivity was measured by Wan der Paul method at 25 °C. Ultrasonically soldered indium pads were used as contacts.

3. Results and discussion

All measured samples were nearly fully dense (>98% TD). The density partially decreased with increasing content of the SiNC precursor in the starting powder. The highest porosity (2%) was observed in the sample SN-5 with the highest content of SiC. Characteristic microstructures of sintered samples are shown in Fig. 1. Microstructure of the sample SN-0 (Fig. 1a) consists of elongated Si₃N₄ grains separated by grain boundary phase. In the case of Si₃N₄ samples doped with the SiNC powder the amorphous precursor crystallized during sintering and formed SiC, Si₃N₄ and free carbon. The stoichiometry of the SiCN precursor suggests that the amorphous SiNC powder yields on crystallisation 66.36 wt.% of Si₃N₄, 27.21 wt.% of SiC and 6.43 wt.% of residual carbon. Increased content of SiC resulted in markedly altered microstructure. Generally, SiC grains and residual carbon formed from the SiNC precursor hindered the grain growth of Si₃N₄ (Fig. 1a–f). Therefore, the sample SN-5 (Fig. 1f) consisted of fine, mostly equiaxed silicon nitride grains with only small fraction of elongated grains.

Location of the *intra*- and *inter*-granular inclusions within Si₃N₄ matrix is shown in Fig. 2. The detailed EELS and EDX

Table 1
Chemical composition of the starting materials

Samples	Chemical composition		
	Si ₃ N ₄ (wt.%)	SiNC (wt.%) (SiC) ^a (wt.%)	Y ₂ O ₃ (wt.%)
SN-0	95	—	5
SN-1	85.5	9.5 (2.6)	5
SN-2	76	19 (5.2)	5
SN-3	66.5	28.5 (7.8)	5
SN-4	57	38 (10.3)	5
SN-5	47.5	47.5 (12.9)	5

^a The fraction of SiC calculated from the amount of added SiNC powder. SiC formed by carbothermal reduction is not considered.

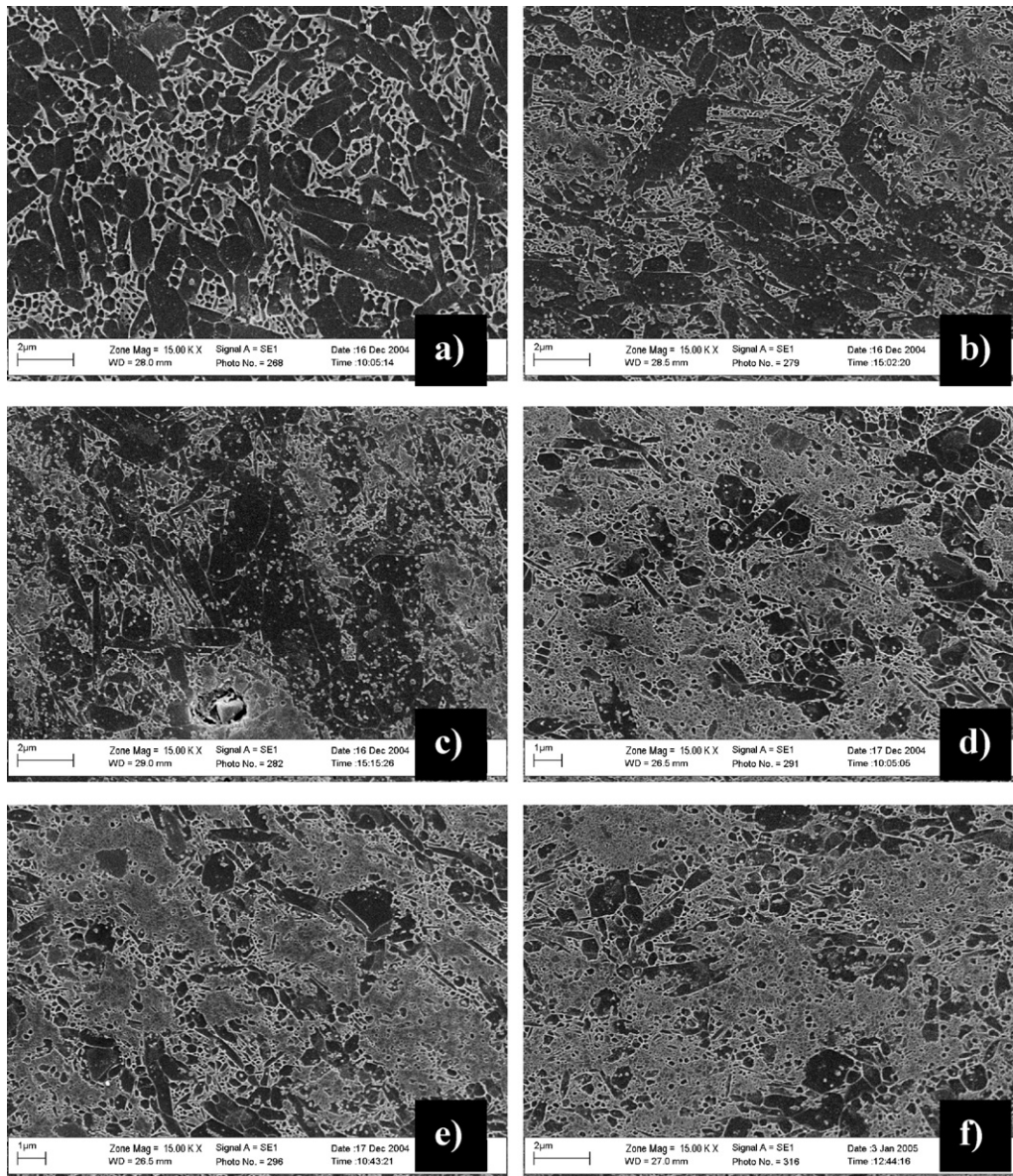


Fig. 1. Characteristic microstructures of (a) SN-0, (b) SN-1, (c) SN-2, (d) SN-3, (e) SN-4, and (f) SN-5 samples.

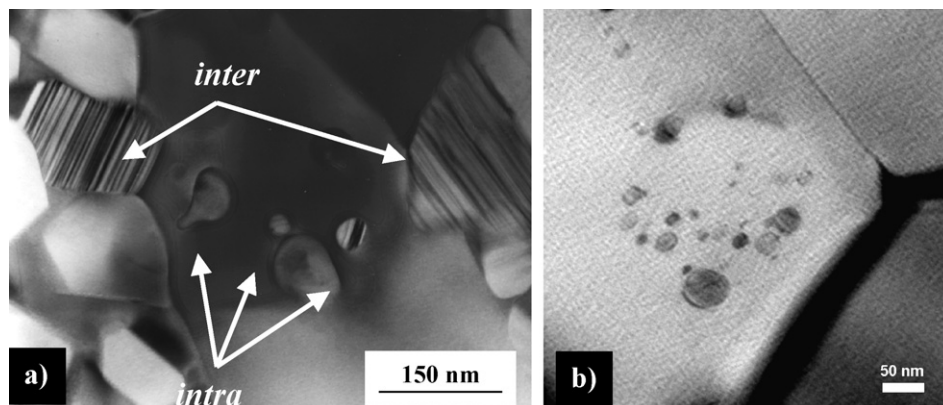


Fig. 2. TEM-bright field image of samples SN-2 with SiC nano-inclusions: (a) *inter* and (b) *inter + intra*.

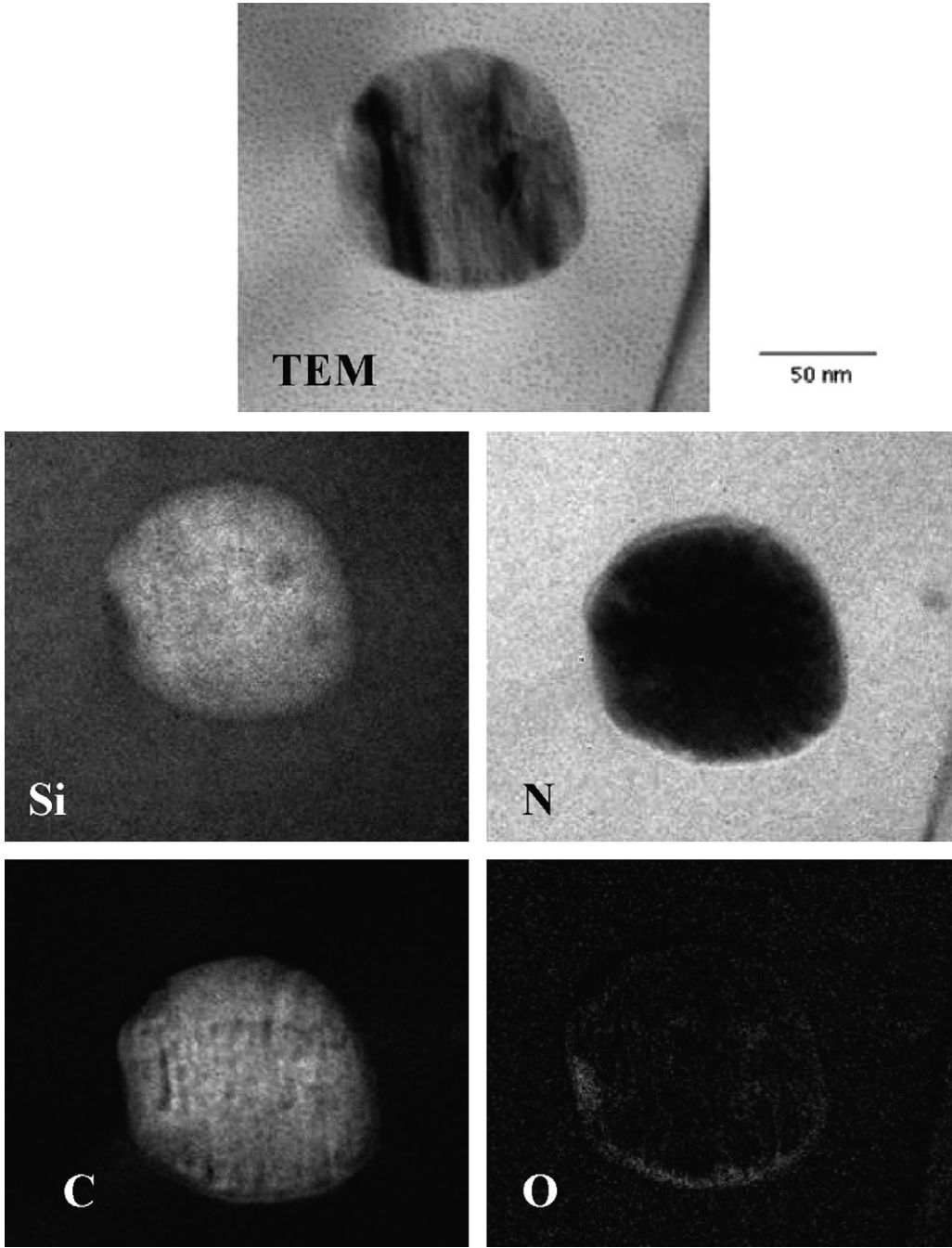


Fig. 3. Chemical analyses of the intra nano-inclusion within the sample SN-2.

analysis confirmed that the chemical composition of the nano-inclusions is equivalent to that of SiC (Fig. 3). The twining of intergranular inclusions was also observed (Fig. 2a), which is the characteristic feature of crystalline SiC. The intra-nano-SiC inclusions could be visualized also by AFM (Fig. 4a) where they appear as brighter spots within darker silicon nitride grains.

The measurements of electrical conductivity revealed the percolation threshold of intergranular SiC particles has been achieved in the composite SN-3 containing estimated 8 wt.% SiC (Table 2). Silicon carbide is a semi-conductor, while silicon nitride is an insulator. The measurements showed that the

Table 2
Electrical resistivity of Si₃N₄/SiC micro/nano-composites

Samples	ρ (Ω m)
SN-0	Non-conductive
SN-1	Non-conductive
SN-2	Non-conductive
SN-3	22.85
SN-4	11.75
SN-5	50.18

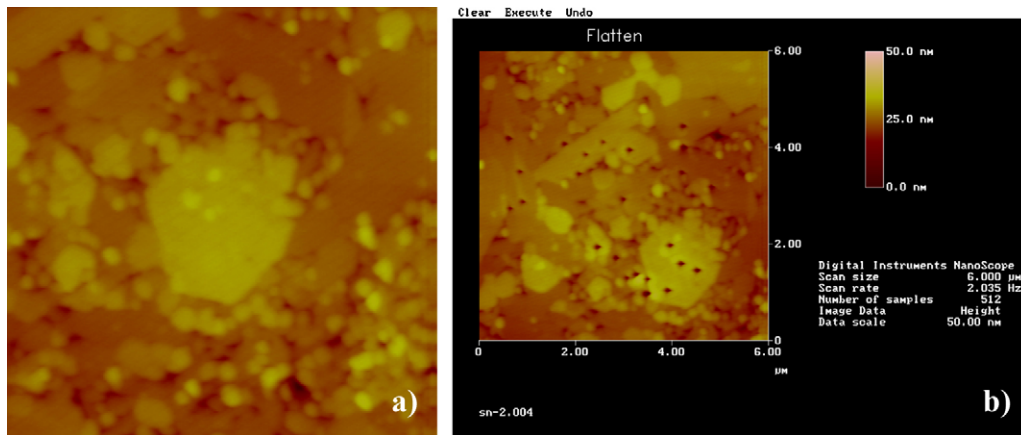


Fig. 4. Characteristic surface of sample SN-2 (a) before (b) after indentation.

samples SN-0, SN-1 and SN-2 are insulators, while the samples SN-3, SN-4 and SN-5 are conductive, which is attributed to formation of conductive path of percolating network of intergranular SiC particles, with possible contribution of free carbon. Higher SiC content enhances the electrical conductivity by increasing the effective cross-section of conductive paths. Increased electrical resistivity of the SN-5 can be attributed to slightly higher residual porosity of this material.

The nano- and macro-hardness of $\text{Si}_3\text{N}_4/\text{SiC}$ composites is shown in Fig. 5. It is known from the literature that the nano-hardness is markedly higher than the macro-hardness owing to the lower indentation load applied. This effect is sometimes described as the indentation size effect.^{12,16} The same effect was observed also in the case of the studied composite materials. The nano-hardness of final composites continuously increases with increasing content of the SiNC additive. In the case of nano-indentations the microstructural features, such as the matrix grain size, are not expected to have a significant influence on the mean values of nano-hardness due to the fact that indents are small and usually occur within a single grain (Fig. 4, the dark triangles are nano-indentation imprints). However, the scatter of data, especially in composites, is expected to be larger due to the presence of *intra*-SiC nano-particles, which can interact with

some of the indents and influence the measured hardness values. The harder *intra*-SiC grains can be nano-indented either directly or together with the surrounding matrix grain, and consequently increase the measured nano-hardness values.

The second mechanism affecting the nano-hardness is the presence of internal stresses within the Si_3N_4 grains due to the thermal expansion mismatch of silicon nitride matrix and *intra*-SiC particles. The calculated value of internal stress can be as high as 1.3 GPa.¹⁷ However, the range of internal stress zones is relatively short, and the decrease of stresses in the direction from the SiC– Si_3N_4 interface is relatively sharp. Moreover, the majority of *intra*-SiC nano-particles were enwrapped in a thin, amorphous oxygen-containing film (Fig. 3). This glassy interlayer can relax the stresses in the course of cooling by plastic deformation. Consequently, the real residual stresses in such system are smaller compared to the theoretical calculations carried out for direct contact of SiC and Si_3N_4 grains. However, some of the examined SiC– Si_3N_4 grain boundaries were free of glass. In this case, both phases were most likely formed by direct crystallisation from the SiNC amorphous precursor, without direct contact with the melt.¹¹ The residual stress balance in Si_3N_4 grains is even more complicated if several SiC nano-inclusions are present within one grain, and the internal stress fields induced by individual SiC nano-grains overlap.

Except of the influence of SiC inclusions in the Si_3N_4 matrix the scatter of measured nano-hardness data can be caused also by the indentation of different crystallographic planes of Si_3N_4 .¹⁸ Dusza et al. showed that the Vickers micro-hardness of prismatic planes is 2120 kg mm^{-2} , while the basal planes had a hardness of only 1330 kg mm^{-2} .¹⁹ This difference is remarkable and should be considered when evaluating the nano-hardness data. However, in this work the influence of crystallographic plane orientation was not evaluated due to the lack of statistically significant set of data.

It was shown that in the case of SiC the diameter of the plastically deformed zone beneath the indent is about five times the lateral width of the observed permanent indent.²⁰ In the case of nano-indentation of Si_3N_4 -based ceramics the situation is most likely very similar. The individual grains were therefore originally indented with the spacing larger than five indent

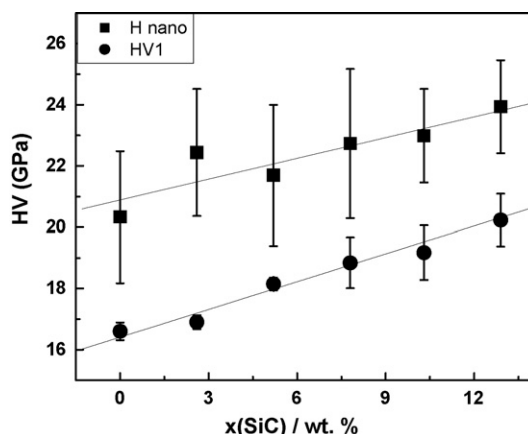


Fig. 5. Comparison of nano- and macro-hardness of $\text{Si}_3\text{N}_4/\text{SiC}$ micro/nano-composites.

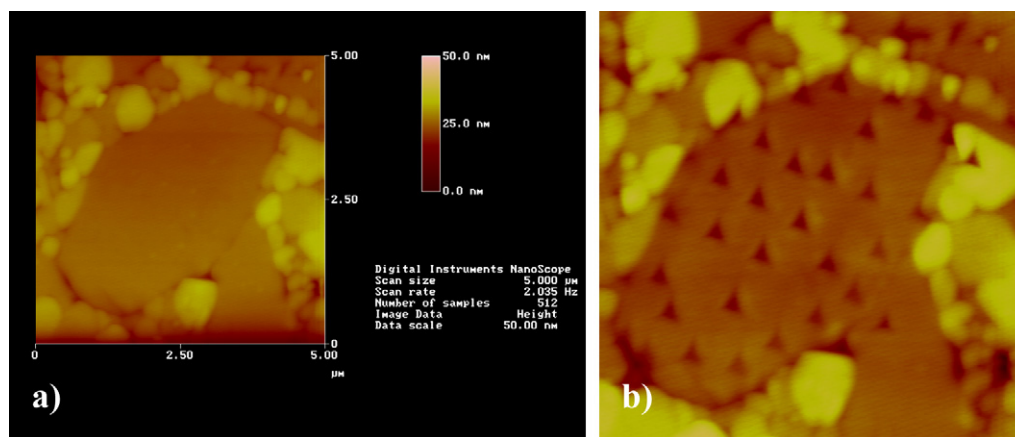


Fig. 6. AFM image of single Si_3N_4 grain in sample SN-1: (a) before and (b) after indentation.

diameters. The measured nano-hardness of an individual grain in the sample SN-1, which did not contain *intra*-SiC particles was 22.5 ± 1.3 GPa. Afterwards, more indentations were made between the existing indents (Fig. 6b), in order to verify the possible influence of plastically deformed zone of the original indents to the indentation response of Si_3N_4 . No significant influence of neighboring indents was observed.

Interesting results were provided by nano-indentation of a single Si_3N_4 grain in the sample SN-2, which contained several SiC inclusions (Fig. 2). The measured hardness was 25.3 ± 1.4 GPa, which is significantly higher than the average nano-hardness of the same sample shown in Fig. 5. In this case the presence of SiC inclusions is likely to cause the deviation from the average value. It is therefore concluded that the presence of *intra*-SiC nano-inclusions has a marked influence on the nano-hardness of individual Si_3N_4 grains.

The hardness of grain boundaries was estimated by direct nano-indentation of interparticle boundaries. However, to carry out the experiment is very difficult due to the fact that the true grain boundary hardness is practically impossible to measure. The thickness of grain boundaries is in the range of only few nanometers, while the triangular imprints are much larger (~ 50 nm). The measured values are therefore always influenced by the surrounding matrix. The grain boundary hardness must be therefore considered only as an approximate estimate, which includes information about the hardness of the thin glassy grain boundary film, the interface between the film and the adjacent matrix grain, and partially also about the hardness of the Si_3N_4 grain itself. The measured “grain boundary nano-hardness” varied for all compositions between 15 and 19 GPa. This indicates that the hardness of grain boundaries is significantly lower than that of the ceramic matrix. Consequently, the grain boundary phase reduces the macro-hardness of the Si_3N_4 /SiC micro/nano-composites. Similar results were reported also for liquid phase sintered SiC.²¹ Nevertheless, the reduction of hardness due to the influence of softer grain boundary phases is expected to vary significantly, depending on the composition of grain boundary phase. In our previous work 10 and 11 we reported on the influence of addition of free C on the composition of grain boundary glass in Si_3N_4 ceramics. Carbon reacts with grain boundary

phases, yielding SiC by carbothermal reduction of silica, and effectively depleting grain boundary glass of SiO_2 . The addition of sufficient amount of C can in extreme case yield virtually silica-free grain boundaries, with positive influence on creep, and possibly, hardness.

Fig. 5 shows that both nano- and macro-hardness follow the same trend. They increase with increasing content of the SiNC additive, i.e. with increasing content of SiC nanoparticles. The sample SN-0 (pure Si_3N_4) with coarse grained microstructure consisting of elongated β - Si_3N_4 grains has lower macro-hardness than the SiC-containing specimens with finer microstructures (Fig. 1). The macro-hardness is likely to increase due to apparent refinement of the Si_3N_4 matrix grains to the size of SiC interparticle spacing.³ Plastic deformation in Si_3N_4 ceramics is the result of formation of intragranular slip bands,²² or by motion of dislocations.²³ The observed microstructure refinement might then increase the hardness by affecting the dislocation mobility due to an increase of the energy barrier for dislocation movement. Similar increase of hardness, attributed to decrease of dislocation mobility due to high density of grain boundaries, was observed in nanocrystalline alumina.²⁴

Although the influence of finer microstructure can be considered as one of the mechanisms responsible for the increase of hardness, the higher hardness of composites must be attributed mainly to the increasing content of SiC inclusions.

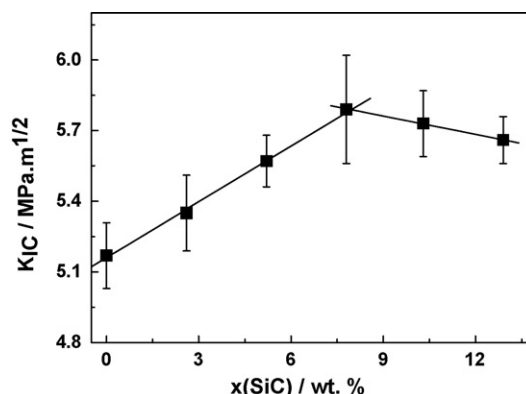


Fig. 7. Fracture toughness of Si_3N_4 /SiC micro/nano-composites.

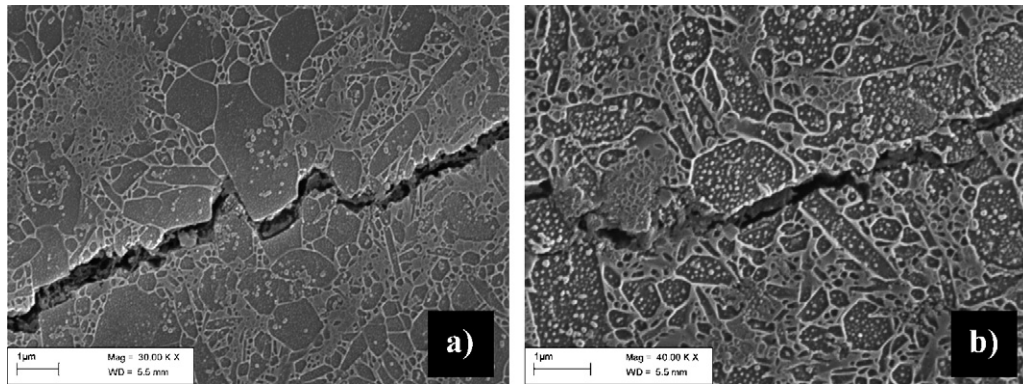


Fig. 8. SEM view of crack paths in sample: (a) SN-3 and (b) SN-4.

Generally, the positive influence of SiC nano-particles (*inter* + *intra*) on the macro-hardness can be attributed to the following aspects:

- (1) SiC nano-inclusions are harder than the Si_3N_4 grains;
- (2) formation of internal stress zones;
- (3) nano-SiC inclusions (*intra*) hinder the movement of dislocations at external load within the Si_3N_4 grains;
- (4) generally finer microstructure, which also decreases the dislocation mobility due to higher grain boundary density.

The indentation fracture toughness of $\text{Si}_3\text{N}_4/\text{SiC}$ micro/nano-composites is summarized in Fig. 7. The fracture toughness increased with increasing content of SiNC amorphous precursor up to 30 wt.% of SiNC (~ 8 wt.% SiC) precursor in the sample. The fracture toughness of the SN-3 specimen was higher than that of the other compositions. At even higher amounts of the SiNC added the fracture toughness slightly decreased. Similar results have been reported for $\text{Si}_3\text{N}_4/\text{SiC}$ composites by Tian et al.²⁵ In their case the reported optimum content of SiC nano-inclusions was 5 vol.%. In this work sample SN-3 with the highest fracture toughness contained approximately 8 wt.% of SiC nano-particles localized both *inter*- and *intra*-granularly.

The observed toughening of $\text{Si}_3\text{N}_4/\text{SiC}$ micro/nano-composite is caused by optimum combination of the microstructure of fine elongated Si_3N_4 grains and the presence of nanometer-sized SiC grains. The elongated Si_3N_4 grains with high aspect ratio increased the fracture toughness by dissipation of fracture energy by crack deflection and bridging in synergy with internal stresses generated by the presence of *intra*-SiC nano-inclusions (Fig. 8a). At 8 wt.% SiC content the percolation threshold of *inter*-SiC particles was achieved, as was determined by the measurement of electrical conductivity. The mechanisms of the action of percolating *inter*-SiC particles on fracture toughness are not clear in this case. On the other hand, sample SN-4 and SN-5 with higher amount of SiC *inter* and *intra* particles (~ 10 and 13 wt.% SiC) exhibits different mechanism of crack propagation (Fig. 8b). In this case trans granular mechanism comparing to the sample SN-3 with *inter* granular have been observed. It seems that higher content of SiC particles then

approximately 8 wt.% (SN-3) has negative effect on fracture toughness due to the changing of crack propagation mechanism. Therefore, it could be concluded that the presence of SiC nano-grains could result in improved mechanical properties but only up to optimized amount of SiC nano-inclusions located in the Si_3N_4 micro-grains. Higher amount of SiC nano-inclusions probably changed the internal integrity (strength) of elongated Si_3N_4 grains, which result to their trans granular fraction. In this case the strength of grain boundary phase becomes higher than the strength of Si_3N_4 grain itself.

4. Conclusions

Dense $\text{Si}_3\text{N}_4/\text{SiC}$ micro/nano-composites were prepared from commercial Si_3N_4 and SiNC amorphous precursor by liquid phase sintering. The SiNC precursor crystallised during sintering to yield SiC, Si_3N_4 and residual carbon. The *in situ* formed SiC nano-particles were located in two different positions: as *inter* and *intra* grain nano-inclusions. The increasing content of the SiC particles increased both the nano- and macro-hardness of $\text{Si}_3\text{N}_4/\text{SiC}$ micro/nano-composites. It is suggested that the SiC nano-inclusions influence the hardness by the presence of the harder SiC nano-particles within the softer Si_3N_4 matrix. Other possible mechanisms of hardness enhancement include microstructure refinement, which might increase the hardness by hindering the dislocation motion within silicon nitride matrix grains.

The maximum fracture toughness $5.8 \text{ MPa m}^{1/2}$ was measured in the sample containing estimated 8 wt.% SiC, which corresponds to the percolation threshold of intergranular SiC particles as determined by measurement of electrical conductivity.

Acknowledgements

Financial support of the Slovak Grant Agency, project nos. VEGA 2/4072/24, VEGA 2/3101/23, grant 2003 ŠO 51/03R 0600/03R 06 03, APVT-51-049702 and Centre of Excellence NANOSMART is gratefully acknowledged. PŠ, ZL and DG acknowledge the financial support of the Alexander von Humboldt Foundation, Germany.

References

- Procházka, J., Karvánková, P., Veprek-Heijman, M. G. J. and Veprek, S., Conditions required for achieving superhardness of ≥ 45 GPa in nc-TiN/ α -Si₃N₄ nanocomposites. *Mater. Sci. Eng. A*, 2004, **384**, 102–116.
- Guicciardi, S., Melandri, C., Medri, V. and Bellosi, A., Effects of testing temperature and thermal treatments on some mechanical properties of a Si₃N₄-TiN composite. *Mater. Sci. Eng. A*, 2003, **360**, 35–45.
- Niihara, K., New design concept of structural ceramics–ceramic nanocomposites. *J. Jpn. Ceram. Soc.*, 1991, **99**(10), 974–982.
- Herrmann, M., Schubert, C., Rendtel, A. and Hübner, H., Silicon nitride/silicon carbide nanocomposite materials. I. Fabrication and mechanical properties at room temperature. *J. Am. Ceram. Soc.*, 1988, **81**(5), 1094–1108.
- Riedel, R., Passing, G., Schonfelder, H. and Brook, R. J., Synthesis of dense silicon-based ceramics at low temperatures. *Nature*, 1992, **355**, 714.
- Galusek, D., Riedel, R. and Balog, M., Polymer-derived Al₂O₃-SiC nanocomposites: preparation route vs. microstructure. *Key Eng. Mater.*, 2005, **290**, 121–128.
- Wang, L., Jiang, W. and Chen, L., Fabrication and characterization of nano-SiC particles reinforced TiC/SiC nano composites. *Mater. Lett.*, 2004, **58**, 1401–1404.
- Luo, Y., Li, S., Pan, W. and Li, L., Fabrication and mechanical evaluation of SiC-TiC nanocomposites by SPS. *Mater. Lett.*, 2003, **58**, 150–153.
- Šajgalík, P., Hnatko, M., Lofaj, F., Hvizdoš, P., Dusza, J., Warbichler, P. et al., SiC/Si₃N₄ nano/micro-composite: processing, RT and HT mechanical properties. *J. Eur. Ceram. Soc.*, 2000, **20**, 453–462.
- Šajgalík, P., Hnatko, M., Lenčič, Z., Warbichler, P. and Hofer, F., SiC/Si₃N₄ nanocomposite prepared by addition of SiO₂ + C. *Z. Metall.*, 2001, **92**(8), 937–941.
- Hnatko, M., Balog, M. and Šajgalík, P., The formation of two types of SiC inclusions in Si₃N₄/SiC nanocomposites. *Key Eng. Mater.*, 2004, **264–268**, 2305–2310.
- Gong, J., Miao, H., Peng, Z. and Qi, L., Effect of peak load on the determination of hardness and Young's modulus of hot-pressed Si₃N₄ by nanoindentation. *Mater. Sci. Eng. A*, 2003, **354**, 140–145.
- Hofer, F. and Warbichler, P., Improved imaging of secondary phases in solids by energy-filtering TEM. *Ultramicroscopy*, 1996, **63**, 21–25.
- Hofer, F., Warbichler, P. and Grogger, W., Nanoanalyse im Elektronenmikroskop. *Spectrum der Wissenschaft*, 1998, **10**, 48–54.
- Shetty, D. K., Wring, I. G., Mincer, P. M. and Clauer, A. H., Indentation fracture of WC-Co cermets. *J. Mater. Sci.*, 1985, **20**, 1873–1882.
- Krell, A., A new look at the influences of load, grain size, and grain boundaries on the room temperature hardness of ceramics. *Int. J. Ref. Met. Hard Mater.*, 1998, **16**, 331–335.
- Šajgalík, P., Hnatko, M. and Lenčič, Z., Properties of silicon nitride/carbide nano/micro-composites—role of SiC nano inclusions and grain boundary chemistry. *Ceramic Materials and Components for Engines*. Wiley-VCH, Weinheim, 2001, pp. 553–558.
- Reimanis, I. E., Suematsu, H., Petrovic, J. J. and Mitchell, T. E., The mechanical properties of single crystal α -Si₃N₄. *Ceram. Trans.*, 1994, **42**, 229–236.
- Dusza, J., Eschner, T. and Rundgren, K., Hardness anisotropy in bimodal grained gas pressure sintered Si₃N₄. *J. Mater. Sci. Lett.*, 1997, **16**, 1664–1667.
- Lankford, J. and Davidson, D. L., Indentation plasticity and microfracture in silicon carbide. *J. Mater. Sci.*, 1979, **14**(7), 1669–1675.
- Balog, M., Hnatko, M., Šajgalík, P., Monteverde, F. and Kečkéš, J., Nano versus macro-hardness of LPS SiC. *J. Eur. Ceram. Soc.*, 2004, **25**, 529–534.
- Milhet, X., Girard, J. C., Demenet, J. L. and Rabier, J., Characterization of room-temperature plastic deformation of β -Si₃N₄ by atomic force microscopy and transmission electron microscopy. *Phil. Mag. Lett.*, 2001, **81**, 623–629.
- Zutshi, A., Haber, R. A., Niesz, D. E., Adams, J. W., Wachtman, J. B., Feber, M. K. et al., Processing, microstructure, and wear behavior of silicon nitride hot-pressed with alumina and yttria. *J. Am. Ceram. Soc.*, 1994, **77**, 883–890.
- Krell, A. and Schädlich, S., Nanoindentation hardness of submicrometer alumina ceramics. *Mater. Sci. Technol. A*, 1996, **209**, 156–163.
- Tian, L., Zhou, Y. and Zhou, W.-L., SiC-nanoparticle-reinforced Si₃N₄ matrix composites. *J. Mater. Sci.*, 1998, **33**, 797–802.